Magazine of Civil Engineering. 2025. 18(4). Article No. 13605

Magazine of Civil Engineering

ISSN
2712-8172

journal homepage: http://engstroy.spbstu.ru/

Research article
UDC 624.21
DOI: 10.34910/MCE.136.5

Probabilistic model for predicting the corrosion-fatigue durability of reinforced concrete railway bridges

G.A. Yefremov ✉ , ***D.A. Shestovitskiy***

Petersburg State Transport University

✉ *frost0077@mail.ru*

Keywords: reinforced concrete, durability, forecasting, numerical methods, service life, corrosion, fatigue of materials, fracture mechanics, probability, railway bridges, Paris law.

Abstract. This study proposes a probabilistic model for assessing the service life of a reinforced concrete railway bridge based on the criterion of corrosion-fatigue durability, taking into account the dynamics of the moving load. Currently, there is no similar methodology approved in the standards of the Russian Federation, as well as in the Eurocodes, while corrosion-fatigue destruction of reinforcement is typical in conditions of chloride-aggressive environments and repetitive loads. In this model, total service life of reinforced concrete superstructure is sum of three periods: corrosion initiation period, crack nucleation period, and crack propagation period. In each period, stochastic variables are specified by probability density functions. As an example of calculating the service life, one of the bridges developed during the design of the Moscow – St. Petersburg High-Speed Railway was chosen. Monte Carlo method was used as the way to modelling the stochastic nature of problem. Failure criteria was the critical crack growth, and crack growth process was modelled using Paris law. The form of the obtained probability density functions for each stage is lognormal; the greatest contribution to the total service life was made by the period of corrosion initiation. In the future, the use of the method will allow the engineer to design structures with a given durability, increase the service life of reinforced concrete bridge spans and more accurately plan funds for repairs of reinforced concrete bridges.

Citation: Yefremov, G.A., Shestovitskiy, D.A. Probabilistic model for predicting the corrosion-fatigue durability of reinforced concrete railway bridges. Magazine of Civil Engineering. 2025. 18(4). Article no. 13605. DOI: 10.34910/MCE.136.5

1. *Introduction*

This study focuses on the degradation of railroad bridge spans under chloride-containing environments. The combination of different effects, in this case chloride ions and repeated load, can lead to the corrosion pit growth and stress concentration in concrete beam reinforcement. Furthermore, repeatable train load can cause nucleation and growth of fatigue crack and rebar failure if crack length will reach its maximum allowed value.

Next some approaches to solving the corrosion-fatigue durability of bridges problem will be presented. For example, condition of working reinforcement under variable load under corrosion conditions is considered in the paper [1], which concludes that the fatigue characteristics of a reinforced concrete girder are reduced as a result of pitting corrosion. European document DuraCrete [2] provides various models of degradation of the span structure under the action of negative climatic factors. S. K. Verma et al. [3] proposes to estimate the service life as the sum of two periods: corrosion initiation and corrosion development period. Some publications are also devoted to the study of bonding of reinforcement with concrete under conditions of corrosion of working reinforcement [4, 5]. One of the first to apply the provisions of fracture mechanics and metal corrosion to calculate the corrosion-fatigue life of a reinforced concrete bridge was E. Bastidas-Arteaga [6]. J. Sun et al. indicated that corrosion, along with temporary loading are the prevailing causes of collapse of reinforced concrete structures [7]. C. Cui et al. consider the negative effects of carbonization together with temporary loading [8]. The authors of a study on prestressed reinforced concrete beams of U-shaped urban rail transit exposed to chloride ions G. Chen et al. [9] indicate that the combined effect of temporary loading and chloride-containing environment can reduce the service life of the span by up to 61.2 %. T. Zhang et al. found that when reinforced concrete beams were jointly exposed to corrosion and repetitive loading, fatigue failure of longitudinal working reinforcement bars occurred [10].

From the above, it can be concluded that, firstly, with coupled action of chloride aggressive environment and repeatable loading, the corrosion-fatigue failure can be typical. Secondly, the problem of service life assessment is complex and currently it is not possible to collect all the developed models into a single methodology and provide a reliable prediction of the service life of reinforced concrete bridge spans. In addition, taking into account the dynamics of span structures is especially important in the calculation of bridges on high-speed highways. The resulting vibrations of the span structure during the passage of a train at high speeds can negatively affect the fatigue life of the span structure, which is not taken into account in the above-mentioned methods. Thus, this task is relevant and requires research. Therefore, in this study, the task was to develop a method for calculating corrosion-fatigue durability that could take into account the dynamic effect of temporary load, as well as the probabilistic natural parameters included in the calculation.

2. Methods

For chloride aggressive environment, pitting corrosion of reinforcement bars is often occurs. It has the most negative effect on the fatigue of reinforcement under the action of train loading [11]-[13]. The appearance of corrosion pits leads to stress concentration in the working reinforcement and fatigue crack initiation. Therefore, when assessing the service life of a span structure by the criterion of corrosion-fatigue durability, it is proposed to distinguish three main periods: the period of corrosion initiation, the period of corrosion pit growth and crack nucleation, and the period of fatigue crack growth until the failure:

$$T = t_{ini} + t_{cn} + t_{cg}. \tag{1}$$

Further we consider separately each of the periods in the probabilistic formulation of the problem.

3. Corrosion Initiation Period

The model of chloride ions penetration into the protective layer of the concrete of the span structure is based on Fick's II law of diffusion [14], [15]. In simplified form for one-dimensional case, it is written as follows:

$$\frac{\partial C}{\partial t} = D \cdot \frac{\partial^2 C}{\partial x^2}, \tag{2}$$

where C – chloride concentration at depth x, at time t; D – diffusion coefficient of chlorides into concrete.

Equation (2) was solved by the finite difference method using Mathcad Prime mathematical package. The scheme for solving equation (2) and the expression for the chloride diffusion coefficient are quite extensive, so we will limit ourselves to references to the corresponding works [6, 16].

The random nature of the parameters included in the equation was taken into account by means of Monte Carlo modelling [17]. This method involves solving this problem N times, each using randomly generated quantities according to their distribution laws. If the number of experiments N is large enough, the modeling results can be considered reliable.

As an example for the calculation, the rigid-framed reinforced concrete span shown in Figs. 1, 2 was used. The design of this overpass was considered as a variant on the Moscow – St. Petersburg High-Speed Railway.

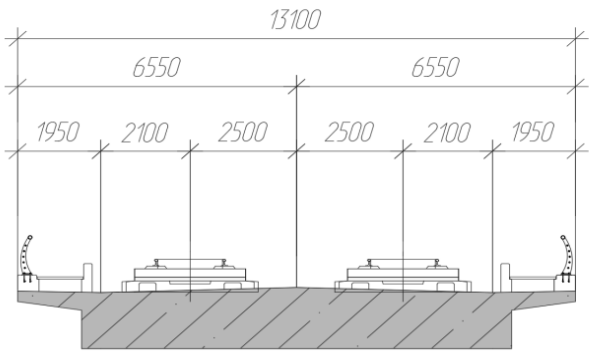

Figure 1. Cross-section of main span.

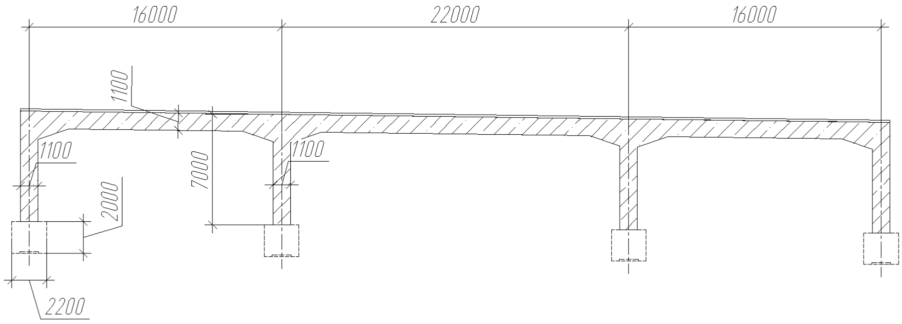

Figure 2. Longitudinal scheme of the bridge.

The initial parameters of the distributions of random variables are given in Table 1.

Table 1. Initial random variables for evaluating corrosion initiation time.

Parameter	Symbol	Probability density function	Expected value	Standart deviation
Water cement ratio	ω_c	Normal	0.4	0.04
Initial diffusion coefficient, m^2/s	$D_{cl,0}$	Normal	$3 \cdot 10^{-11}$	$0.6 \cdot 10^{-11}$
Activation energy of the diffusion process, kJ/mol	U	Normal	41.8	4.18
Protective layer of concrete, mm	c_t	Normal	50	7.5

The initial constant values are given in Table 2.

Table 2. Initial constant variables for evaluating corrosion initiation time.

Parameter	Symbol	Value
Number of experiments	N	1000
Maximum monthly average temperature, °C	T_{max}	26
Minimum average monthly temperature, °C	T_{min}	–5
Maximum monthly average humidity	W_{max}	0.79
Minimum average monthly humidity	W_{min}	0.72
Surface concentration of chlorides, kg/m^3	C_s	1.5
Binding constant	α	0.1185
Binding constant	β	0.09

The variability of air temperature and humidity is taken into account using the following equation:

$$f_{T,W}(t) = \frac{\varphi_{max} + \varphi_{min}}{2} + \frac{\varphi_{max} + \varphi_{min}}{2} \sin(2\pi t) + \lambda_{T,W}, \tag{3}$$

where φ_{max} is the maximum value of the parameter (temperature, humidity); φ_{min} is the minimum value of the parameter (temperature, humidity); t is time in years, $\lambda_{T,W}$ is a random parameter having normal distribution, mathematical expectation equal to 0 and standard deviation of temperature 3 °C and humidity 0.01. The graphs of these functions (3) are shown in Fig. 3. The sinusoids $T_0(t)$ and $W_0(t)$ are the mean values of these functions without considering monthly deviations, $T(t)$ and $W(t)$ take into account the random fluctuations of ambient temperature and humidity.

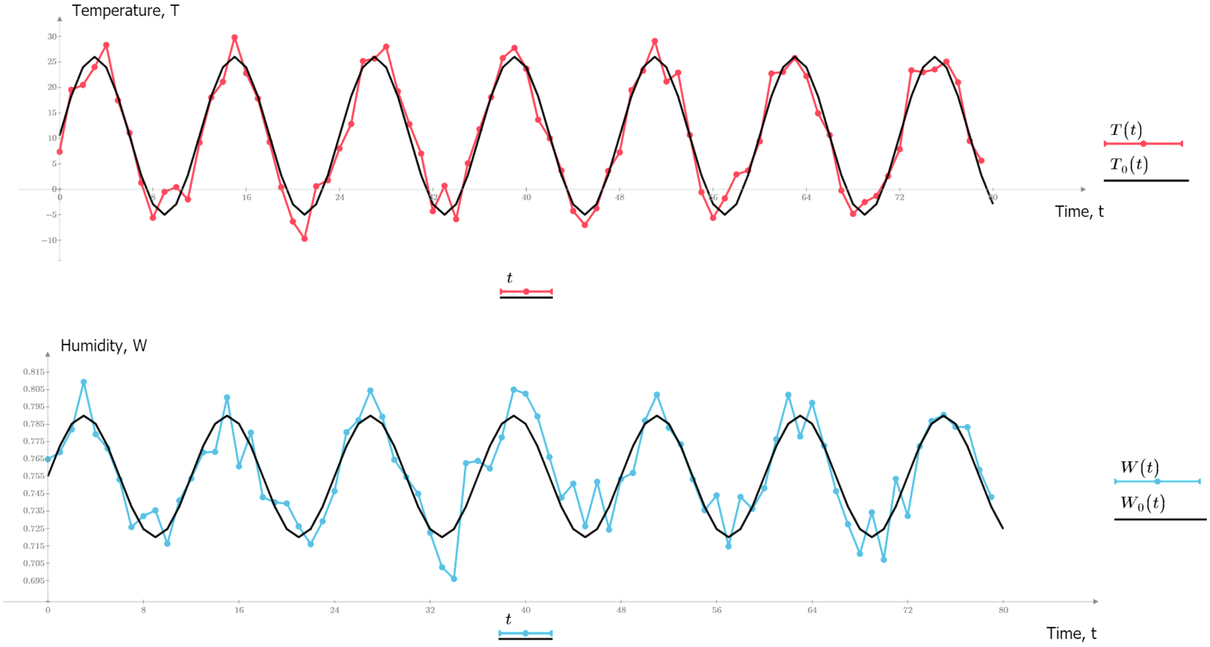

Figure 3. Plots of humidity and temperature dependence in deterministic and probabilistic form.

As a result of modeling 1000 iterations, in each of them, profiles of chloride concentration distribution along the depth of reinforced concrete span were obtained and the time, in which chloride concentration at the depth of concrete protective layer will reach the critical value, was calculated. The final function of the corrosion initiation time distribution is shown in Fig. 4.

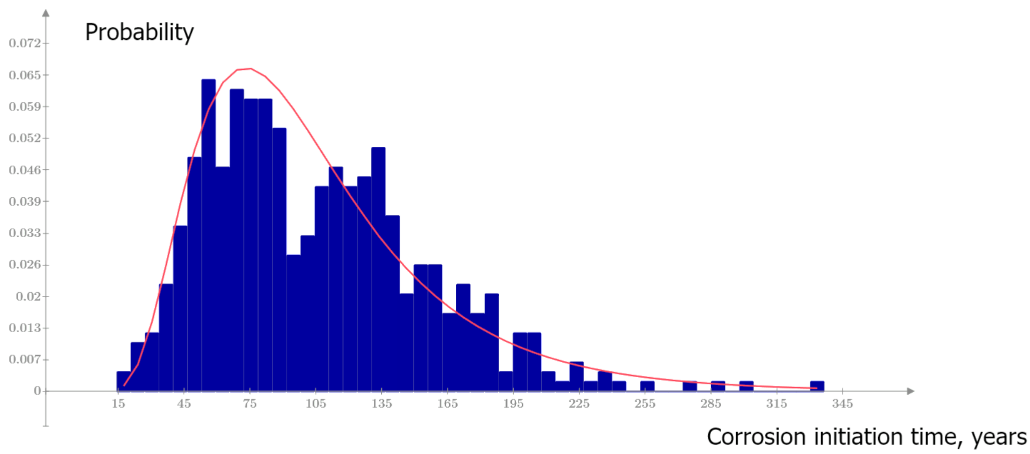

Figure 4. Distribution histogram and probability density distribution curve of corrosion initiation time of the working reinforcement of the span structure.

The graph shows the distribution histogram of the Monte Carlo simulation results and the theoretical probability density curve, which corresponds to a lognormal distribution with a mean value in these conditions of 105.4 years, standard deviation of 55.9 years. The value, below which the corrosion initiation time does not fall with a 95 % probability or 5th percentile, is 41 years.

4. Time of Corrosion Pit Growth and Fatigue Crack Initiation

The second step in the total service life calculation is the calculation of the time, in which the stress concentration at the corrosion pit will lead to fatigue crack nucleation. The study [18] uses the following statement to calculate this time: for crack nucleation, it is necessary for the growth rate of the corrosion pit to coincide with the growth rate of the conditional crack at a point equal to the depth of corrosion development. In other words:

$$\frac{da}{dt} = \frac{dp}{dt}. \tag{4}$$

The left side of equation (4) represents the growth rate of the fatigue crack and is calculated using Paris's law [19, 20]:

$$\frac{da}{dt} = C_p \Delta K^{m_p} f, \tag{5}$$

where a is the crack size; C_p, m_p are coefficients depending on the material; ΔK is the stress intensity factor range [21]; f is the frequency of train loading (number of cycles per year).

The right part of equation (4) is the growth rate of the corrosion pit, calculated by the formula [22]:

$$p(t) = 0{,}00116a \int i_{corr}(t)\,\mathrm{dt}. \tag{6}$$

Thus, the growth time of the corrosion cavity before fatigue crack initiation is determined by equating (5) and (6) and solving with respect to t. The initial constants and random variables used in the solution are tabulated below.

Table 3. Initial random variables for evaluating crack nucleation time.

Parameter	Symbol	Probability density function	Expected value	Standart deviation
Corrosion initiation time, years	t_{ini}	Log-Normal	105.4	55.9
Concrete cover layer, mm	c_t	Normal	50	7.5
Paris law constant	C	Log-Normal	$1.8 \cdot 10^{-11}$	$1.118 \cdot 10^{-11}$
Paris law constant	m	Log-Normal	3.34	0.2
Water/cement ratio	ω_c	Normal	0.4	0.04
Pitting coefficient	α	Log-Normal	5.65	0.215

Table 4. Initial constant variables for evaluating crack nucleation time.

Parameter	Symbol	Value
Diameter of rebar, mm	d	32
Train load frequency, train/day	f	10
Average stress range in reinforcement	$\Delta\sigma$	75
Number of experiments	N	10000

The results of the Monte Carlo simulation in the form of a plot of the probability density function of the crack nucleation time are shown in Fig. 5.

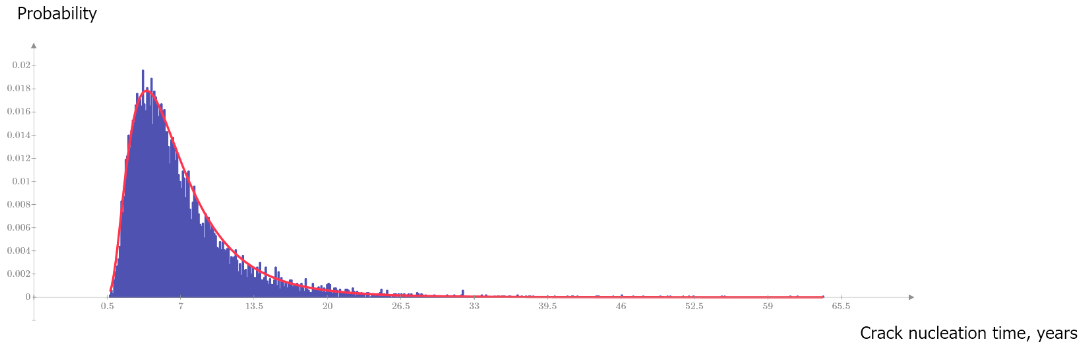

Figure 5. Distribution histogram and distribution density curve of the probability density function of crack initiation time in the working reinforcement of the span structure.

As in the case of corrosion initiation time, the fatigue crack initiation time is a lognormal distribution with mathematical expectation of 7 years, standard deviation of 4.6 years, and 5th percentile of 2.2 years.

5. Time of Crack Growth to Critical Value

The crack growth time to critical value is determined using Paris's law, see formula (5).

In this case, to calculate the stress intensity factor, it is also necessary to determine the stress difference arising from the train load. For this purpose, a nonlinear deformation model can be used; its basic provisions are given in [23]. The random nature of the parameters included in the calculation was also taken into account, see Table 5. The forces in the cross-section were found by dynamic calculation in the program complex realizing the finite element method [24]. The dynamic calculation is necessary to obtain the spectrum of the force factor and to take into account the contribution of each vibration of the spanning structure to the fatigue crack growth.

Table 5. Initial random variables to calculate stresses in reinforcement bars

Parameter	Symbol	Probability density function	Expected value	Standart deviation
Cross-section width, m	b	Normal	10.1–11.6	0.202–0.232
Cross-section height, m	h	Normal	1.64	0.016
Tensile reinforcement area, m^2	A_{s1}	Normal	0.05466	0.00137
Compressed reinforcement area, m^2	A_{s2}	Normal	0.03537	0.00088
Concrete Young's modulus, MPa	E_b	Normal	36000	2880
Steel Young's modulus, MPa	E_s	Normal	200000	6000
Cross-section center of gravity location, m	h_g	Normal	0.862	0.00862

Table 6. Initial constant variables to calculate stresses in reinforcement bars.

Parameter	Symbol	Value
Tensile strength of reinforcement, MPa	R_s	350
Design value of concrete compressive strength, MPa	R_b	20
Ultimate reinforcement strain	ε_s	0.025
Ultimate concrete compressive strain	ε_b	0.0035
Number of cross-section parts	n	30
Number of experiments	N	1000
Critical crack value, mm	a_{cr}	0.74·d

Similar to the previous steps, the probability distribution of the crack growth period was obtained and the 5th percentile was cut off, which amounted to 5.5 years (Fig. 6).

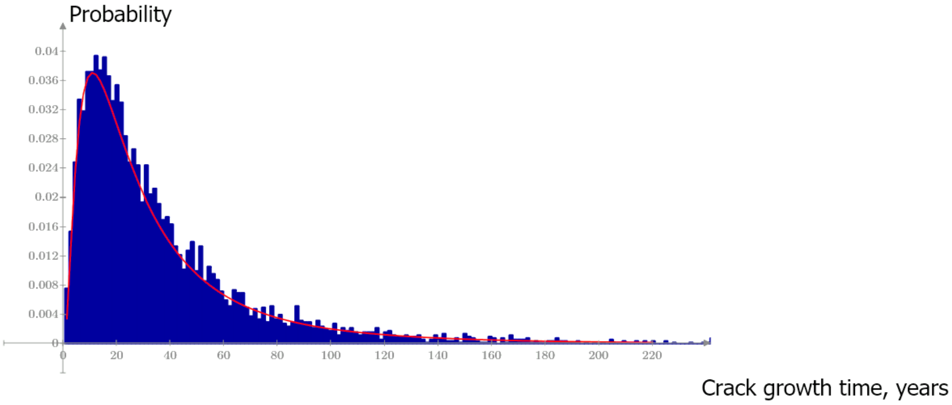

Figure 6. Distribution histogram and probability density distribution curve of crack growth time-to-failure probability in the working reinforcement of the spanwise structure.

6. Results and Discussions

To calculate the final service life of the structure, Monte Carlo simulation of the sum of three periods was performed, each of the periods was generated as a random variable based on the calculations performed. The final nature of the service life distribution can be seen in the figure below:

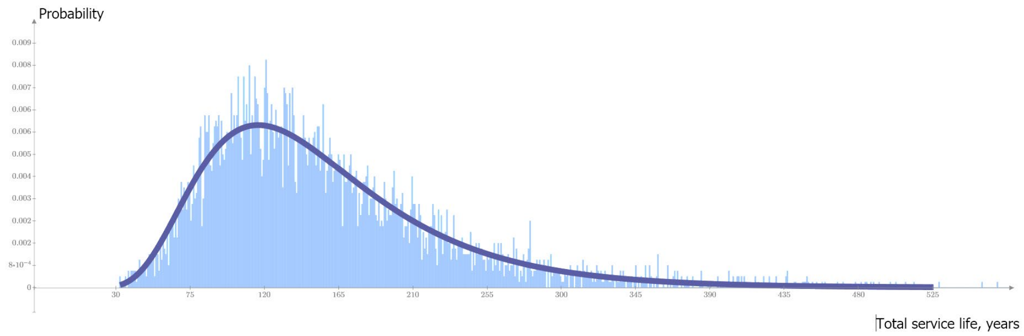

Figure 7. Distribution histogram and probability density distribution curve of the service life probability of the span structure based on the corrosion-fatigue life criterion.

Below is a summary table with the results of calculating the time of each of the periods and the total service life of the span structure.

Table 7. Results of calculating the time of crack initiation and growth before failure.

Parameter	Symbol	Probability density function	Expected value	Standart deviation	5th percentile
Corrosion initiation time, years	t_{ini}	Log-normal	112.5	62.8	42.5
Fatigue crack nucleation time, years	t_{cn}	Log-normal	7	4.6	2.2
Fatigue crack growth time, years	t_{cg}	Log-normal	38.2	43	5.5
Total bridge span service life, years	T	Log-normal	158.5	75.04	69.5

If we compare results with those available in various sources, we obtain a generally similar expected value of design service life, for example, in paper [25] for traffic load frequency 50/day and low-aggressive environment design service life of 157 years was obtain with standart deviation 57 years. The service life probability distribution density, obtained by the authors, also lognormal. However, with an increase in the frequency of load and the aggressiveness of the environment, the average service life drops to 20–40 years.

The authors [8] investigated corrosion-fatigue durability under carbonization and repeatable loading. Results show that the design service life of a 6-meter reinforced concrete plate superstructure is 162.1 years. However, the authors also conclude that corrosion-fatigue durability decreases by 67 % if traffic frequency increases from 1000 vehicles/day to 7000 vehicle/day.

A study of train loading coupled with aggressive environmental influences carried out by the authors [9] also showed a high corrosion-fatigue durability of 164.8 years with a low concentration of chloride ions and low load intensity, however, an increase in the concentration of chloride ions (from 2.5 kg/m^3 to 5.87 kg/m^3) reduced this value by 50 %, and an increase in train load (from 109 trains/day to 721 trains/day) – by 30 %.

In general, the possible dispersion of final results among different authors is associated with a large number of initial parameters of the model; the configurations of spans, the type and magnitude of the traffic load, climatic parameters, materials used, etc.

7. Conclusion

According to the results of the conducted research, we can conclude the following:

1. The corrosion initiation period, fatigue crack initiation time, crack growth time to failure, and the total service life of the span structure obey a lognormal distribution. The hypothesis that the sample from the Monte Carlo simulation results belong to the lognormal distribution is tested using Pearson's $\chi 2$ criterion of agreement, the critical value of the $\chi 2$ criterion is accepted for a significance level of 5 %.
2. The greatest contribution to the corrosion-fatigue durability is made by the corrosion initiation period, which indicates that if the working reinforcement is sufficiently protected from corrosion, it will be possible to significantly extend the service life of the structure. On the contrary, if the train moving load is significant and, for example, the protective layer is insufficient, the failure of the reinforcement can occur in a relatively short period of time.
3. The modern engineer has powerful tools for direct dynamic analysis of the structure, which, according to the proposed methodology, allows to estimate the contribution of each vibration of the span to the growth of fatigue crack, which can be used at the stage of design of artificial structures.
4. The service life of a structure, like everything in our world, has a probabilistic nature. In practice, probabilistic calculations are complicated and it is not reasonable to repeat them for each structure. Based on the results of this study, it is possible to calculate the reliability coefficient for the service life of the span structure for the example selected for the calculation. However, to develop a system of reliability coefficients for different initial data, further research on the influence of the variation of initial parameters on the statistical parameters of the service life of the structure is necessary.

References

1. Tamrazyan, A.G. Fatigue Behavior of Flexural Reinforced Concrete Beams under Corrosion Conditions. Reinforced Concrete Structures. 2024. 2(6). Pp. 24–36. DOI: 10.22227/2949-1622.2024.2.22-34
2. DuraCrete. Modelling of Degradation: Probabilistic Performance based Durability design of Concrete Structures. Document BE-1347. R4-5. 1998.
3. Verma, S.K., Sudhir, S.B., Saleem, A. Estimating Residual Service Life of Deteriorated Reinforced Concrete Structures. American Journal of Civil Engineering and Architecture. 2013. 1(5). Pp. 92–96. DOI: 10.12691/ajcea-1-5-1
4. Thajuddeen, H., Karthik, M. Fatigue Bond Life of Reinforced Concrete Beams with Low Reinforcement Corrosion. Proceedings of International Structural Engineering and Construction. 2024. 11(2). Pp. 1–6. DOI: 10.14455/ISEC.2024.11(2).STR-18
5. Zhou, H., Qi, X., Lin, Z., Filippo, M., Liu, J., Ma, C., Xing, F. An experimental study on bond behaviors of reinforced concrete under fatigue loading and corrosion. Structural Concrete. 2022. 24(1). Pp. 504–520. DOI: 10.1002/suco.202200684
6. Bastidas-Arteaga, E., Bressolette, P., Chateauneuf, A., Sanchez-Silva, M. Probabilistic lifetime assessment of RC structures under coupled corrosion-fatigue deterioration. Structural Safety. 2009. 31(1). Pp. 84–96. DOI: 10.1016/j.strusafe.2008.04.001
7. Sun, J., Ding, Z., Huang, Q. Corrosion fatigue life prediction for steel bar in concrete based on fatigue crack propagation and equivalent initial flaw size. Construction and Building Materials. 195. 2019. Pp. 208–217. DOI: 10.1016/j.conbuildmat.2018.11.056
8. Cui, C., Song, L., Liu, J., Yu, Z. Corrosion-Fatigue Life Prediction Modeling for RC Structures under Coupled Carbonation and Repeated Loading. Mathematics. 2021. 9. Article no. 3296. DOI: 10.3390/math9243296
9. Chen, G., Wang, M., Cui, C., Zhang, Q. Corrosion-Fatigue Life Prediction of the U-Shaped Beam in Urban Rail Transit under a Chloride Attack Environment. Materials. 2022. 15(17). Article no. 5902. DOI: 10.3390/ma15175902
10. Zhang, T., Zhang, X., Li, P., Li, H., Li, X., Zou, Y. Experimental Research on Fatigue Performance of Reinforced Concrete T-Shaped Beams under Corrosion. Fatigue Coupling Action. Materials. 2023. 16(3). Article no. 1257. DOI: 10.3390/ma16031257
11. Stewart, M.G. Time-dependent reliability of deteriorating reinforced concrete bridge decks. Structural Safety. 1998. 20(1). Pp. 91–109. DOI: 10.1016/S0167-4730(97)00021-0

12. Wang, H., He, S., Yin, X., Cao, Z. Experimental Study on Fatigue Performance of Reinforced Concrete Beams in Corrosive Environment with Cyclic Loads. Structural Durability & Health Monitoring. 2020. 14(2). Pp. 95–108. DOI: 10.32604/sdhm.2020.06595
13. Zhang, W., Song, X., Gu, X., Li, S. Tensile and fatigue behavior of corroded rebars. Construction and Building Materials. 2012. 34. Pp. 409–417. DOI: 10.1016/j.conbuildmat.2012.02.071
14. Liao, J., Wang, Y., Sun, X., Wang, Y. Chloride Penetration of Surface-Coated Concrete: Review and Outlook. Materials. 2024. 17(16). Article no. 4121. DOI: 10.3390/ma17164121
15. Sun, J., Jin, Z., Chang, H., Zhang, W. A review of chloride transport in concrete exposed to the marine atmosphere zone environment: Experiments and numerical models. Journal of Building Engineering. 2024. 84. Article no. 108591. DOI: 10.1016/j.jobe.2024.108591
16. Shalyy, E.E., Kim, L.V., Leonovich, S.N. Reinforced Concrete under Influence of Carbonization and Chloride Aggression: Probable Model of Service Life Calculation. Bulletin of Belgorod State Technological University named after. V. G. Shukhov. 2018. 6. Pp. 5–14. DOI: 10.12737/article_5b115a5ef027c2.76676320
17. Novák, D., Strauss, A., Novák, L., Lehký, D., Šomodíková, M., Lipowczan, M., Slowik, O., Doležel, J., Pukl, R., Sattler, F., Apostolidi, E. Nonlinear probabilistic structural assessment: Findings from Austrian and Czech bridges. EUROSTRUCT 2023: European Association on Quality Control of Bridges and Structures: Digital Transformation in Sustainability. 2023. 6(5). Pp. 1242–1251. DOI: 10.1002/cepa.2195
18. Chen, G., Wan, K., Gao, M., Wei R., Flournoy, T. Transition from pitting to fatigue crack growth modeling of corrosion fatigue crack nucleation in a 2024-T3 aluminum alloy. Materials Science and Engineering. 1996. 219(1–2). Pp. 126–132. DOI: 10.1016/s0921-5093(96)10414-7
19. Paris, P.C., Erdogan, F. A Critical Analysis of Crack Propagation Laws. Journal of Basic Engineering. 1963. 85. Pp. 528–533. DOI: 10.1115/1.3656900
20. Salah el din, A.S., Lovegrove, J.M. Fatigue of cold worked ribbed reinforcing bar – a fracture mechanics approach. International Journal of Fatigue. 1982. 4(1). Pp. 15–26. DOI: 10.1016/0142-1123(82)90016-0
21. Murakami, Y., Nisitani, H. Stress intensity factor for circumferentially cracked round bar in tension. Transactions of the Japan Society of Mechanical Engineers. 1975. 41. Pp. 360–369. DOI: 10.1299/kikai1938.41.360
22. Liang, M., Jin, W., Yang, R., Huang, N. Predeterminate model of corrosion rate of steel in concrete. Cement and Concrete Research. 2005. 35(9). Pp. 1827–1833. DOI: 10.1016/j.cemconres.2004.10.005
23. Trekin, N.N., Alekseytsev, A.V., Bobrov, V.V., Domarova, Ye.V. Raschet zhelezobetonnykh izgibayemykh konstruktsiy na osnove nelineynoy deformatsionnoy modeli. [Calculation of reinforced concrete bendable structures based on a nonlinear deformation model]. Moscow: MISI-MGSU Publishing, 2023. 63 p.
24. Efremov, G.A., Myachin, V.N., Shestovitskiy, D.A. Influence of cyclic loading on corrosion-fatigue life of concrete bridges superstructure. The Siberian Transport University Bulletin. 2023. 66(3). Pp. 51–59. DOI: 10.52170/1815-9265_2023_66_51
25. Bastidas-Arteaga, E. Reliability of Reinforced Concrete Structures Subjected to Corrosion-Fatigue and Climate Change. International Journal of Concrete Structures and Materials. 2018. 12. Article no. 10. DOI: 10.1186/s40069-018-0235-x

Information about the authors:

Gleb Yefremov*,*
ORCID: https://orcid.org/0000-0001-9311-3765
E-mail: frost0077@mail.ru

Dmitriy Shestovitskiy*, PhD in Technical Sciences*
E-mail: shestovitsky@mail.ru

Received 02.11.2024. Approved after reviewing 26.05.2025. Accepted 09.06.2025.